The British Journal of Radiology, 84 (2011), 81–91

PICTORIAL REVIEW

Clinical presentations and imaging findings of neuroblastoma beyond abdominal mass and a review of imaging algorithm

[1]C M CHU, FRCR, [1]D D RASALKAR, FRCR, [3]Y J HU, MD, [2]F W T CHENG, MRCP, [2]C K LI, FRCP and [1]W C W CHU, MD

[1]*Department of Diagnostic Radiology and Organ Imaging,* [2]*Department of Pediatrics, Prince of Wales Hospital, The Chinese University of Hong Kong, Hong Kong SAR, China and* [3]*Imaging Centre, ZhangJiaGang No.1 People's Hospital, ZhangJiaGang City, Jiangsu Province, P.R. China*

ABSTRACT. Neuroblastoma is one of the most common malignant neoplasms in childhood. The most common clinical presentation of this tumour is abdominal mass. However, affected children may have various clinical presentations as a result of disseminated metastatic disease or associated paraneoplastic syndromes at the time of diagnosis. In this article we have outlined the imaging findings in seven patients with ''extra-abdominal'' presentation of neuroblastoma and the pitfalls in making the correct diagnosis. The purpose of this pictorial review is to alert the general radiologist to the possible presentations of this common childhood malignancy to derive early detection and diagnosis.

Received 27 January 2010
Revised 4 May 2010
Accepted 27 May 2010

DOI: 10.1259/bjr/31861984

Neuroblastoma is the most common solid extracranial tumour in infants and children. It represents approximately 7% of all cases of childhood cancer and results in about 15% of cancer deaths in children [1]. Neuroblastoma arises from primitive neuroblasts of the embryonic neural crest, and therefore can occur anywhere within the sympathetic nervous system [2]. The most common site of the primary tumour occurs within the abdomen (65%). About half of these tumours arise from the adrenal medulla. Other common sites of neuroblastoma include the neck, chest and pelvis [3].

The classic clinical presentation of neuroblastoma is well recognised by paediatric radiologists [4]; however, medical professionals or radiologists working in local hospitals may not be aware of the atypical manifestations of this tumour. As prompt diagnosis and treatment may help to increase survival rates and minimise irreversible damage, especially to the neural system, it is important for both clinicians and radiologists to be aware of some of the less common manifestations of this tumour.

In this article, we illustrate the ''extra-abdominal'' clinical presentations and imaging findings of seven cases of abdominal neuroblastoma diagnosed in our hospital, a tertiary Children Cancer Centre in Hong Kong, over the past 10 years.

Address correspondence to: Winnie C W Chu, Department of Diagnostic Radiology and Organ Imaging, Department of Pediatrics, Prince of Wales Hospital, The Chinese University of Hong Kong, Hong Kong SAR, China. E-mail: winnie@med.cuhk.edu.hk

Case reports

Seven patients were included in this pictorial review (Figure 1-7). All of them had primary neuroblastoma within the abdomen, but the initial clinical presentation was extra-abdominal. Two of them presented with bone pain with non-specific radiographic and MRI findings at the symptomatic joints. Both patients were initially under orthopaedic care with provisional diagnosis of juvenile idiopathic arthropathy and septic arthritis, respectively. Four patients presented with swelling in the head and neck regions: one patient with scalp nodules, two patients with periorbital swelling and one patient with mandibular swelling. These ''lumps and bumps'' were subsequently found to be bony metastases from abdominal neuroblastoma. One patient presented with diarrhoea and was initially treated for gastroenteritis. This symptom was retrospectively found to be related to the paraneoplastic syndrome of neuroblastoma. Two of the above children subsequently developed lower limb weakness related to intraspinal extension of the abdominal neuroblastoma. The correct diagnosis was first proposed when cord compression was found on urgent MRI examination.

A summary of demographic data, clinical presentation, staging, treatment and outcome of all patients is given in Table 1.

Discussion

The presenting signs and symptoms of neuroblastoma are highly variable with a broad spectrum. They are related to the site of the primary tumour, presence of metastases

Table 1. Summary table of demographic data, clinical presentation, staging, treatment and outcome of the patients

Case	Age	Sex	Presenting symptoms	Site of primary tumour	Disease extent/site of metastases	Stage	Treatment and clinical outcome
1 (Figure 1)	6 years	M	Acute onset of left shoulder pain	Right adrenal	Retroperitoneal lymphadenopathy Widespread bone and bone marrow metastases (left shoulder involving the clavicle, scapula and proximal humerus, lower thoracic and lumbar spine, iliac bones, sacrum, proximal femurs)	IV	Intensive chemotherapy followed by peripheral stem cell transplant Died at age 8 years with multiple brain metastases
2 (Figure 2)	3 years	M	Left hip pain, limping gait and fever	Left adrenal	Extradural compression of spinal cord at T9/10 Widespread bone metastasis (proximal femoral metaphysis and pelvic ischium), bone marrow, paraspinal and pleural involvement	IV	Intensive chemotherapy followed by peripheral stem cell transplant Bony relapse at age 5 years
3 (Figure 3)	14 months	F	On and off fever for 2 weeks and several nodules over the scalp	Left adrenal	Left renal, retroperitoneal, pelvic and inguinal nodal metastases, bone metastasis (right parietal skull)	IV	Chemotherapy, tumour debulking and radiotherapy In remission. No recurrence at age 2 years 6 months
4 (Figure 4)	8 months	M	Diarrhoea for 5 days, followed by progressive lower limb weakness with decrease in movement	Left adrenal	Intraspinal extension and extradural compression of the cord from the level of T10-L1/2	III	Urgent laminectomy, debulking surgery and chemotherapy In remission. No recurrence at age 4 years. Paraplegic with neurogenic bladder.
5 (Figure 5)	7 months	F	Watery eye discharge and gradual increase in eye swelling extending into bitemporal region	Right adrenal	Bone metastasis to bilateral orbit and bilateral greater wings of the sphenoid bone	IV	Chemotherapy and resection of right adrenal tumour In remission. No recurrence at age 10 years
6 (Figure 6)	2 years 6 months	F	Difficulty in walking for 3 weeks. Right submandibular swelling for 1 week.	Left adrenal	Bone metastases (right mandible and left femur)	IV	Chemotherapy, debulking resection of primary tumour, right segmental mandibulectomy, followed by radiotherapy and peripheral stem cell transplant Died at age 4 years with multiple brain metastases
7 (Figure 7)	1 year 5 months	M	Bilateral periorbital swelling and proptosis	Left adrenal	Liver metastasis. Bony metastasis to bilateral orbits, temporal bones, sphenoid wings and maxillae	IV	Chemotherapy, debulking of primary tumour, radiotherapy and peripheral stem cell transplantation Died at age 4 years with multiple brain metastases

Table 2. Summary table of clinical presentations [4]

Anatomical site of the primary tumour	
Head and neck	Unilateral palpable mass, Horners syndrome (ptosis, miosis, anophthalmos, anhydrosis)
Orbit and eye	Exophthalmoses, periorbital ecchymoses (raccoon eyes), palpable masses, edema of conjunctiva, papilledema, strabismus, anisocoria. Opsoclonus (involuntary rapid eye movements in all directions of gaze)
Chest	Upper thoracic tumours: dyspnoea, pulmonary infections, dysphagia. Lower thoracic tumours: usually no symptoms
Abdomen and pelvis	Abdominal mass, Anorexia, vomiting, pain, constipation and urinary retention
Paraspinal regions	Back pain, paraplegia, weakness, areflexia or hyperreflexia in lower extremities accompanied with muscle atrophy, scoliosis. Bladder and anal sphincter dysfunctions
Bones	Pain, limping
Lymph nodes	Enlarged cervical mass
Non-specific constitutional symptoms	
Anorexia, lethargy, pallor, weight loss, abdominal pain, weakness, irritability	
Paraneolastic syndrome	
Owing to excessive catecholamine (VMA/HVA)	Sweating, flushing, pallor, headache, palpitation
Owing to vasoactive intestinal peptides (VIP)	Dehydration, hypokalaemia and abdominal distention, secretory diarrhoea, failure to thrive (Kerner–Morrison syndrome)
Acute myoclonic encephalopathy (opsoclonus-myoclonus [OM] syndrome)	Opsoclonus (dancing eyes syndrome), myoclonus (irregular jerking of muscles of limbs and trunk)

and any associated paraneoplastic syndromes [2]. A summary of the spectrum of clinical signs is given in Table 2 [5]. Around 40% of patients present with signs and symptoms owing to localised disease. Paraspinal tumours in the thoracic, abdominal and pelvic regions occur in 5–15% of patients, and these can extend into the neural foramina causing symptoms related to compression of nerve roots and the spinal cord [6–8]. In this case series, Cases 4 and 6 presented with bilateral lower limb weakness owing to intraspinal extension of the neuroblastoma causing spinal cord compression. Two major paraneoplastic syndromes are commonly seen in patients with localised tumours. Secretion of vasoactive intestinal peptide can result in diarrhoea [2]; this symptom was present in Case 4 of this series. Diarrhoea usually resolves after tumour removal [9]. Most of the patients with abdominal neuroblastoma in this series had a sizable primary tumour. Medical professionals should be aware of the possible symptoms and signs related to this relatively common paediatric neoplasm. Quick abdominal examination supplemented by ultrasound screening can enable a correct diagnosis and facilitate optimal management of the child.

Extra-abdominal presentations of neuroblastoma

About 50% of patients present with evidence of haematogenous metastases to distant sites such as cortical bone, bone marrow, liver and non-regional lymph nodes.

Skeletal metastases occur in up to 60% of cases with a variable radiological appearance [1]. Skeletal lesions in long bones may present radiographically as osteolytic focus with or without periosteal reaction, lucent horizontal metaphyseal line or vertical linear radiolucent streaks in the metadiaphysis. Some skeletal lesions may present as a pathological fracture. Vertebral collapse might

Table 3. International guidelines for diagnosis and imaging follow-up [9]

Tumour site	Recommended tests
Primary tumour	CT and/or MRI scan with 3D measurements; MIBG scan if available
Metastatic sites	
Bone marrow	Bilateral posterior iliac crest marrow aspirates and trephine (core) bone marrow biopsies required to exclude marrow involvement. A single positive site documents marrow involvement. Core biopsies must contain at least 1 cm of marrow (excluding cartilage) to be considered adequate
Bone	MIBG scan; ^{99}Tc scan required if MIBG scan negative or unavailable, and plain radiographs of positive lesions are recommended
Lymph nodes	Clinical examination (palpable nodes), confirmed histologically. CT scan for non-palpable nodes (3D measurements)
Abdomen/liver/chest	CT and/or MRI scan with three dimensional measurements. Anteroposterior and lateral chest radiographs. CT/MRI necessary if chest radiograph positive, or if abdominal mass/nodes extend into chest

3D, three-dimensional; MIBG, ^{18}I-metaiodobenzylguanidine.

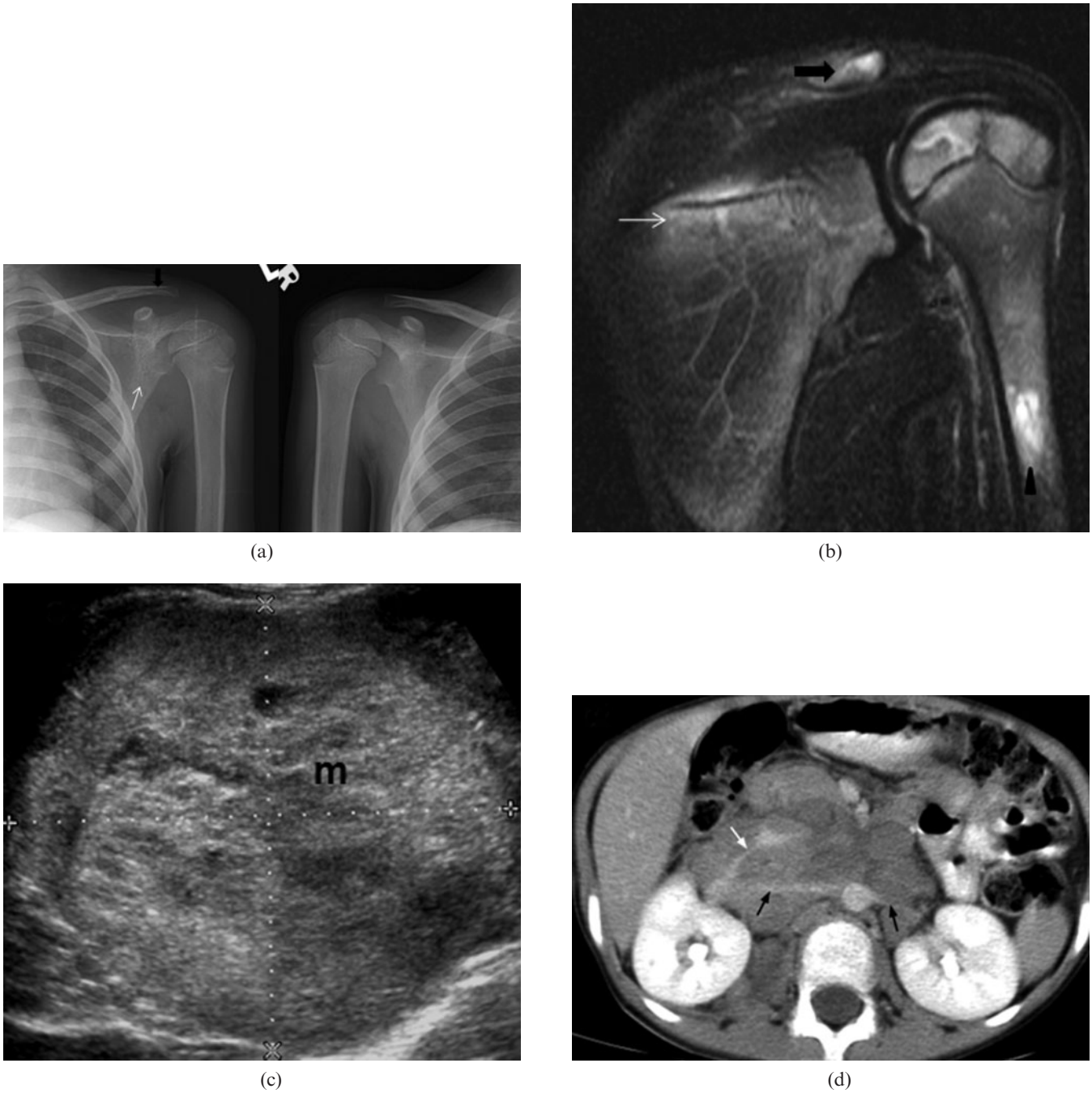

(a) (b) (c) (d)

Figure 1. Right adrenal neuroblastoma in a 6-year-old boy who presented with left shoulder pain, anaemia and raised erythrocyte sedimentation rate (ESR). He was initially misdiagnosed as having juvenile idiopathic arthropathy. (a) Plain radiograph. When compared with the normal right side there is periarticular osteopenia of the left shoulder involving the clavicle (black arrow) and scapula (white arrow). (b) Coronal fat-saturation T_2 weighted image of left shoulder shows multifocal increased marrow signal in the lateral end of the clavicle (black arrow), the scapula (white arrow) and the proximal humerus (arrowhead). A small amount of joint effusion is also evident. (c) Transverse ultrasound image of the abdomen shows a large heterogeneous mass at the right adrenal bed (M). It was confirmed as neuroblastoma after ultrasound-guided biopsy. **(d)** Contrast-enhanced axial CT image shows a large, poorly enhancing soft-tissue mass with classical vascular encasement of both renal arteries (black arrows) and right renal vein (white arrow).

be seen in spinal metastases while metastases to the cranium often manifest as widening of the cranial suture lines owing to subjacent dural metastases. Early skeletal lesions may be missed when cortical destruction is limited as in Case 1 and 2 of this series. MRI is more sensitive for detection of bony lesion; however, the findings might be misinterpreted as other infective/inflammatory causes that share non-specific MRI features. In Case 1 the patient presented with left shoulder pain and fever. He was initially misdiagnosed with juvenile idiopathic arthropathy as the clinical presentation overlapping with arthritic symptomatology. In Case 2 the patient presented with a limp and left hip pain. His MRI was misinterpreted as septic arthritis owing to the

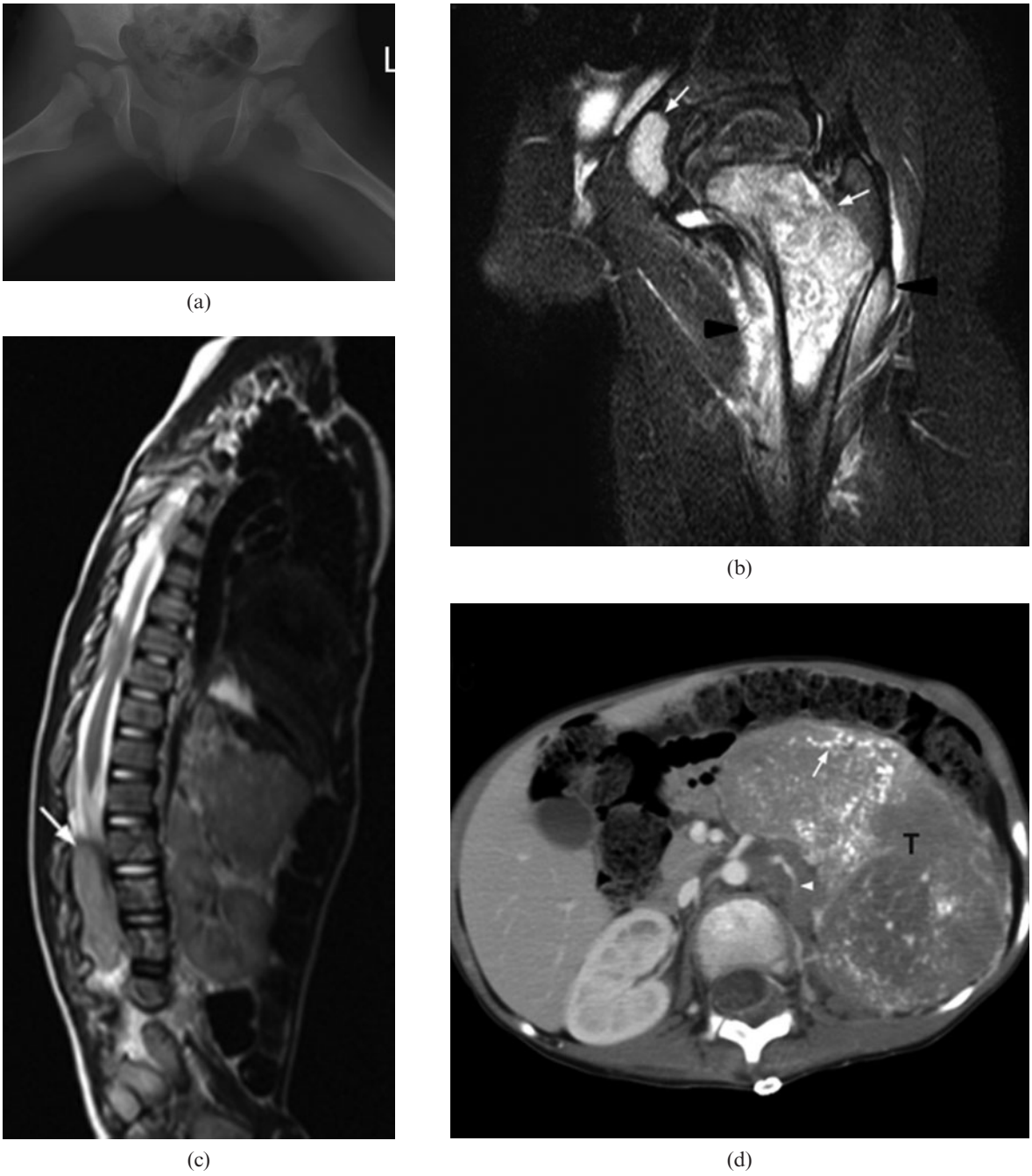

(a) (b) (c) (d)

Figure 2. A 3-year-old boy with Stage IV neuroblastoma who presented with left hip pain, limp and fever. A blood test showed elevated chronic reactive protein (CRP). He was initially misdiagnosed as having septic arthritis. (a) Plain radiography of both hips shows no obvious bony destruction of the left proximal femur when compared with the asymptomatic right side. (b) Coronal MR T_2 weighted image with fat saturation of the left hip reveals marked T2 hyperintense signal of proximal femoral metaphysic and acetablum (white arrows) together with signal change in the surrounding muscle (arrow heads). This was misinterpreted as osteomyelitis at the initial study. (c) MRI of the spine and abdomen shows distal cord and cauda equina compression by a large abdominal soft-tissue mass with intraspinal extension (white arrow). (d) Contrast-enhanced axial CT image shows a large heterogeneously enhancing soft-tissue mass (T) with extensive intratumoural calcifications (white arrow) in the left side abdomen. The left kidney (not shown) is displaced inferiorly and the left renal vein (arrowhead) is encased. Ultrasound biopsy confirmed neuroblastoma.

presence of joint effusion, soft-tissue oedema and concurrent fever. Subsequent examination confirmed that their musculoskeletal symptoms were related to bone metastases.

Neuroblastoma also has an unexplained tendency to metastasise to the bony orbit and as a result periorbital ecchymoses (''raccoon eyes'') and proptosis are features of disseminated neuroblastoma [2]. Cases 5 and 7 in this series presented with periorbital swelling and raccoon eyes. Proptosis was also evident in the latter patient. In Case 3, the patient presented with scalp nodules. The diagnosis of bony metastases in the above cases became obvious when bone destruction and characteristic periosteal reaction were demonstrated on CT images.

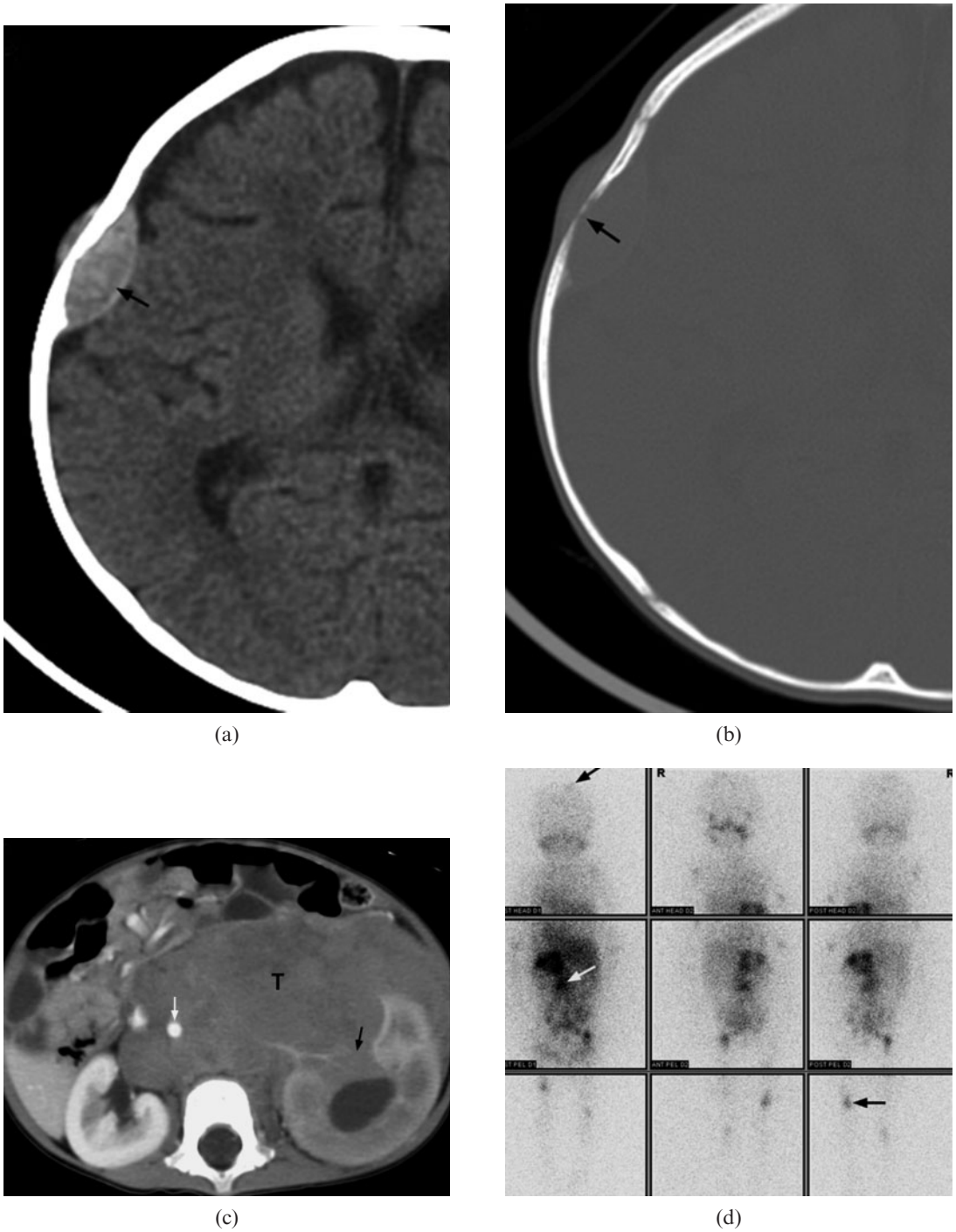

(a) (b) (c) (d)

Figure 3. A 14-month-old girl with Stage IV neuroblastoma who presented with scalp nodules and on/off fever for two weeks. (a,b) Axial CT of brain demonstrates a lentiform soft-tissue mass in right parietal bone (black arrow) associated with bony erosion. (c) Contrast-enhanced axial CT image of abdomen shows a large soft-tissue mass (T) at the left sided retroperitoneal space. The tumour encases the abdominal aorta (white arrow) and invades the left kidney (black arrow). (d) Metaiodobenzylguanidine scintigraphy demonstrates multiple foci of abnormal tracer uptake (arrows) in the abdomen, skull and appendiceal skeleton.

Imaging algorithms in neuroblastoma

Successful planning of individual patient therapy requires precise delineation of the local extent of the neuroblastoma and evaluation of distant metastases. CT, MRI and bone scintigraphy are the primary imaging modalities used in staging disease in children with neuroblastoma. The imaging protocol might vary from institution to institution. Brodeur et al [10] has published the revised criteria for neuroblastoma diagnostic work up based on experience with the International Neuroblastoma Staging System (INSS) and International Neuroblastoma Response Criteria (INRC). The imaging tests recommended for assessment of the extent of the disease are listed in Table 3. One major modification proposed in Bordeur's paper [10] is that CT scans or MRI (but not ultrasound) are recommended to evaluate the abdomen. It is recommended that three-dimensional measurements

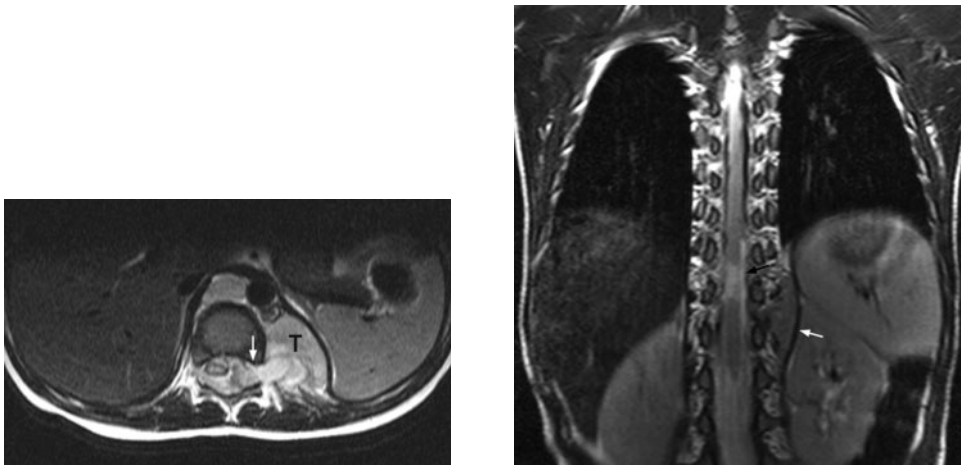

(a) (b)

Figure 4. An 8-month-old boy with Stage III neuroblastoma who presented with diarrhoea for 5 days and was treated for gastroenteritis. Subsequently, he was found, by the mother, to have deterioration in standing power. (a) Axial T_2 weighted MRI shows compression of the cord by a left paravertebral tumour (T) with intraspinal extension via the neural foramina (white arrow). (b) Follow-up coronal T_2 weighted MRI reveals residual small left paravertebral tumour after completed treatment (white arrow). There is a short segment of myelomalacia (black arrow) at the distal cord. The patient suffers from a persistent neurological deficit.

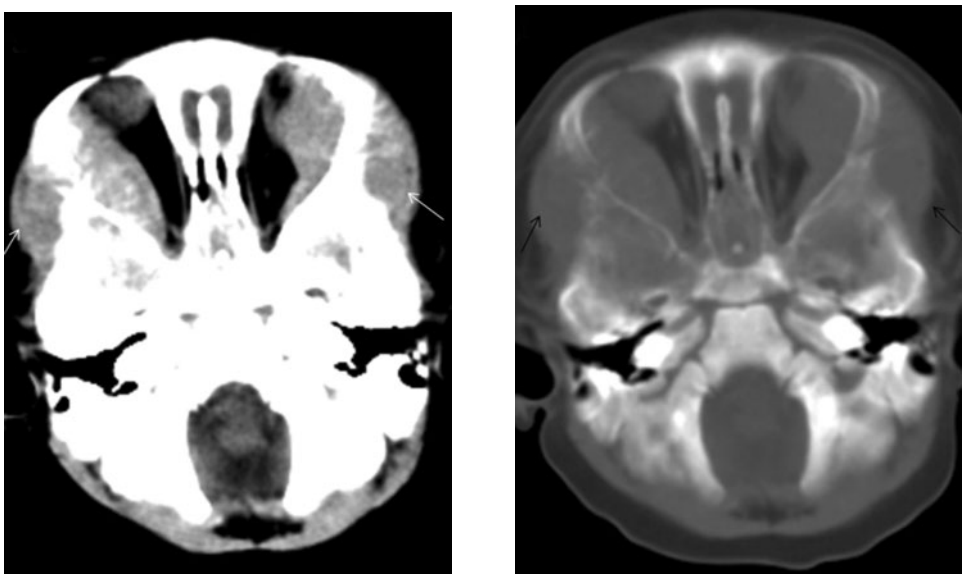

(a) (b)

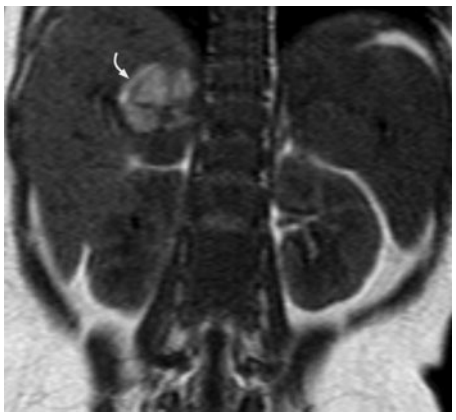

(c)

Figure 5. Stage IV neuroblastoma in a 7-month-old girl who presented with watery eye discharge and orbital swelling for 10 days. (a,b) CT image of the brain demonstrates bilateral intraorbital soft-tissue masses (white arrows) with bony orbit involvement (black arrows). It extends laterally into the subcutaneous soft tissues. (c) Coronal T_1 weighted MRI shows a heterogeneous mass in which the high signal intensity area corresponds to tumoural haemorrhage (curved arrow).

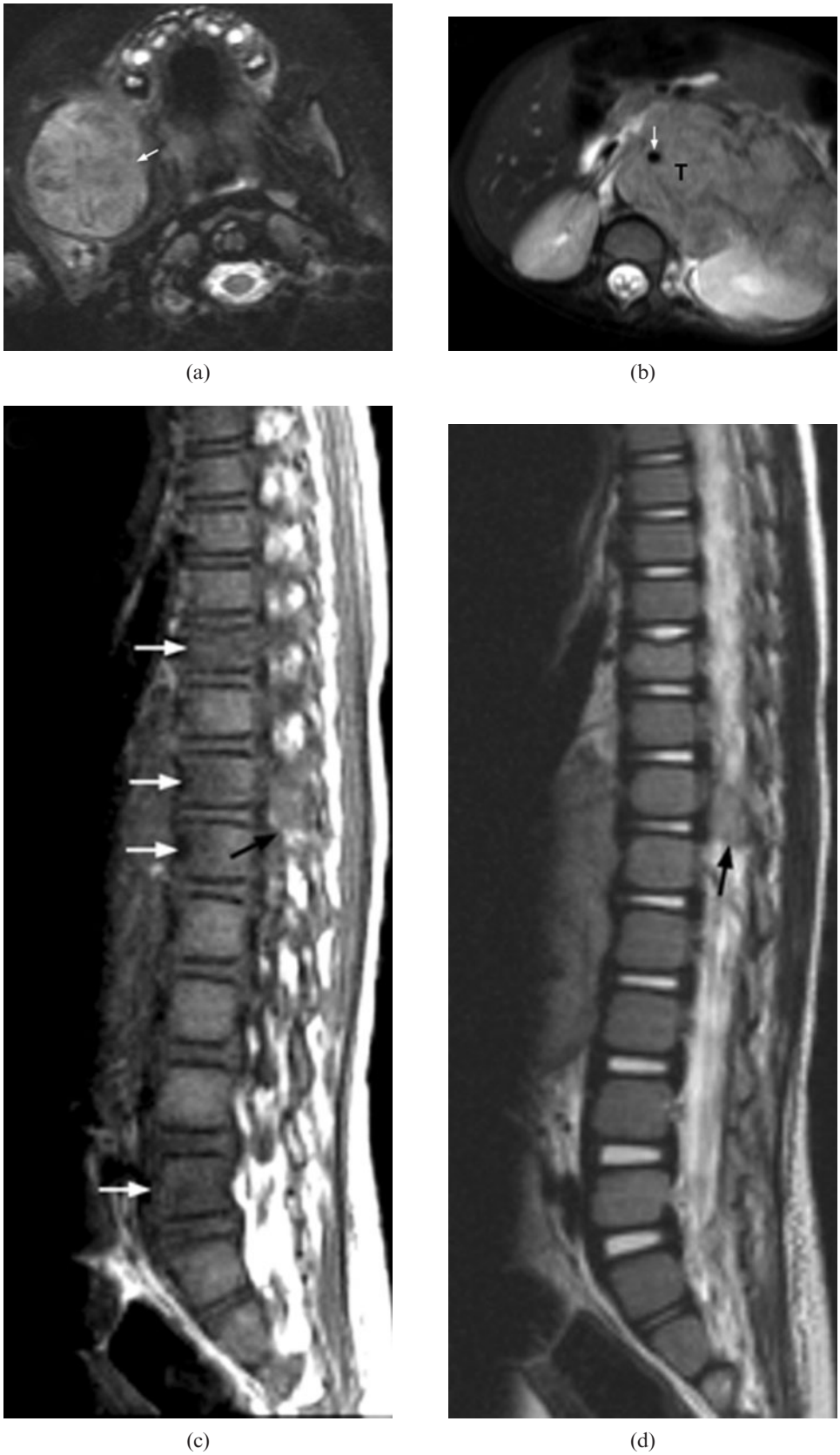

Figure 6. Stage IV neuroblastoma in a 30-month-old girl who presented with right facial swelling. (a) Axial fat-saturation T_2 weighted image shows a large tumour involving the body, angle and coronoid process of the right side of the mandible (arrow). (b) Axial T_2 weighted MRI shows a large left adrenal tumour (T) encasing the abdominal aorta (white arrow). (c) Sagittal T_1 weighted image and (d) T_2 weighted image reveal direct extension of tumour into the spinal canal via the left T12/L1 intervertebral foramen (black arrow). There are multiple foci of abnormal signal intensity in the vertebral bodies at the level of T10, T12, L1 and L5 (white arrows).

(a)

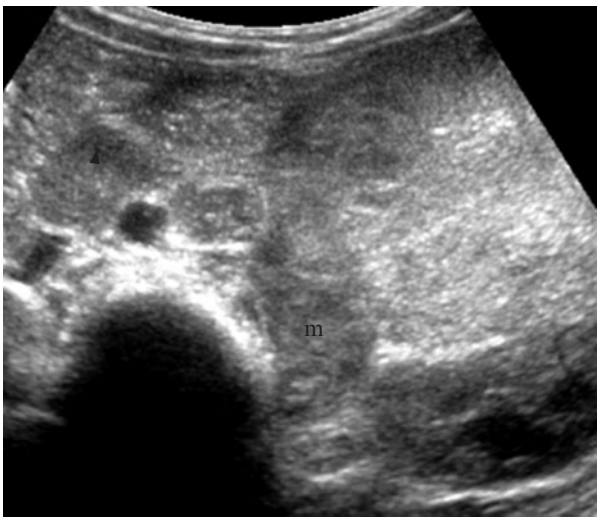

(b)

(c)

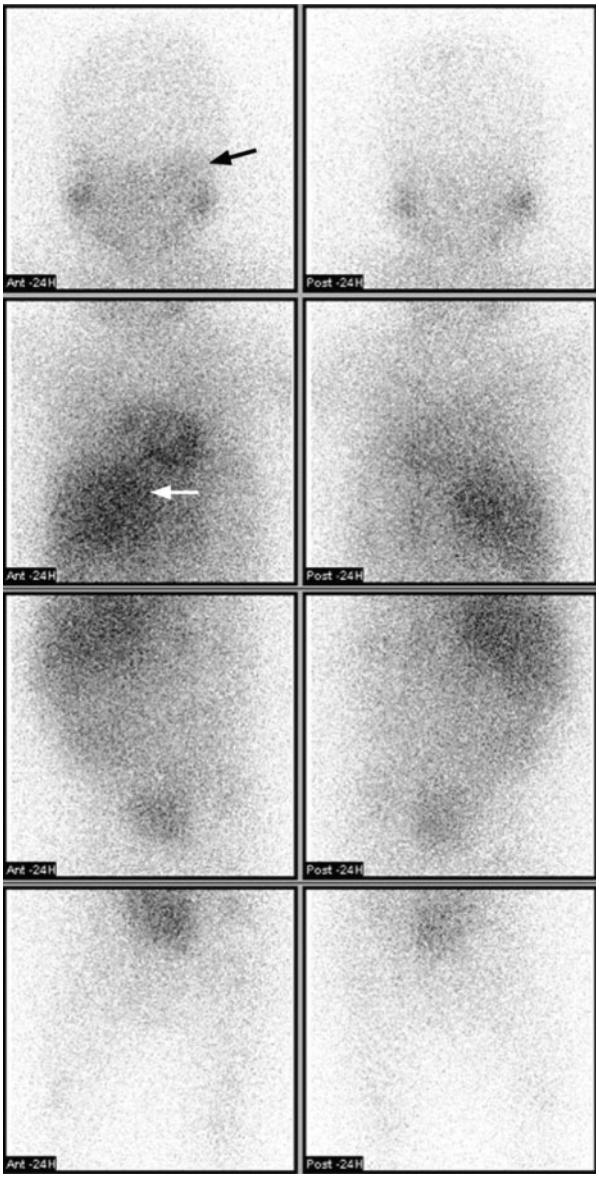

(d)

Figure 7. A 17-month-old boy with Stage IV neuroblastoma who presented with fatigue and periorbital swelling. (a) Plain radiography of the skull shows ill-defined lucency (arrow) over left periorbital bone. (b) Transverse ultrasound of abdomen shows an echogenic mass (m) at left adrenal bed with enlarged para-aortic lymph node (arrowhead). (c) Axial post-contrast CT of the abdomen shows a large mass (T) in the retroperitoneum with small amount of tumoural punctuate calcifications (arrows). The major vessels are encased. Diffuse liver metastases (black arrows) are also noted. (d) Metaiodobenzylguanidine scintigraphy shows increase in tracer uptake over left orbital region (black arrow). There is also intense uptake in the primary abdominal tumour (white arrow).

of the primary tumour and large metastases should be obtained by CT or MRI to determine response to treatment, while ultrasound may be a useful modality for interim assessments. Recently, MRI has supplemented CT for the staging of neuroblastoma [11–13]. In small series, MRI has also been shown to be more sensitive in the detection of local disease [14, 15]. MRI is better for paraspinal lesions and is essential when assessing intraforaminal extension of the tumour and its potential for cord compression [2]. MRI is also superior to CT for characterising epidural extension, leptomeningeal disease and for the detection of bone marrow metastases [16]. However, many district hospitals may not have the facilities for paediatric MRI, particularly in the age group prevalent for neuroblastoma, in whom general anaesthesia is often required. Contrast-enhanced CT is therefore the most commonly used modality for disease staging for neuroblastoma worldwide. CT alone has been reported to be 82% accurate in revealing tumour extent [10].

Metaiodobenzylguanidine (MIBG), which is taken up by tumours derived from the neural crest, has excellent sensitivity (>90%) and near-absolute specificity in the context of neuroblastoma owing to its tumour-specific uptake [17]. A recent study shows that MIBG single photon emission CT (SPECT) bridges the gap between planar MIBG scintigraphy and diagnostic CT [18]. SPECT is particularly useful in cases where there is difficult differential anatomy to distinguish between bowel loops and eventual involved lymph nodes on CT, and in cases when CT reading is impaired by anatomical distortion after surgery or irradiation. SPECT also enhances the diagnostic certainly for small foci, which are overlooked by CT. ^{111}In-diethylenetriaminepentaacetic acid (DTPA)-octreotid scan (somatostatin receptor analogue) yields prognostic information for neuroblastoma [19]. Positive octreotide scintigraphy indicates high level of somatostatic-2 (SST2) receptor gene expression within neuroblastoma and is correlated with a favourable clinical outcome [20]. However, MIBG scinitgraphy is more sensitive than octreotide scintigraphy for detection of neuroblastoma, therefore both studies have a complementary role in initial diagnostic workup [21].

In a review by McHugh and Pritchard [22], the importance of differentiating stage IVS (which has a Stage I/II primary tumour and dissemination limited to the liver, skin and/or bone marrow) and Stage IV (which has metastases to distant lymph nodes, bones, bone marrow, liver and/or other organs) diseases have been emphasised. Several investigators have reported the presence of MIBG scan-negative, bone scan-positive sites of metastatic neuroblastoma [17]. To omit bone scanning may result in incorrect staging in up to 10% of cases. Supplementary bone scintigraphy reportedly increases the accuracy to 97% [10]. Bone scintigraphy has been traditionally used to survey for occult bony metastases [23, 24]. In the setting of confirmed neuroblastoma and multiple or diffuse abnormalities detected on bone scintigraphy, the positive findings should be regarded as highly suggestive of bone metastases even if plain radiography of the abnormal sites is unrevealing. Ideally, MIBG and bone scintigraphy should be done in all children with neuroblastoma at diagnosis to help decide the correct treatment strategy.

Positron emission tomography-CT (PET-CT) has gained importance in staging child cancer. Fluorodeoxyglucose (FDG) PET-CT has the advantage over the standard imaging modalities of characterising tumours both anatomically and metabolically. In a recent study, 113 paired 18-fluoro-FDG PET studies and ^{123}I-MIBG scintigraphy were compared for their diagnostic accuracy in neuroblastoma [25]. In general, FDG can better delineate disease extent in the chest, abdomen and pelvis and is superior in depicting Stage I and II neuroblastoma. MIBG is better for detection of bone and marrow metastases and is overall superior in evaluation of Stage IV neuroblastoma, especially during initial chemotherapy. However, in patients with tumours that weakly accumulate ^{123}I-MIBG, PET studies provide important information during staging and at major decision points during therapy, such as before stem cell transplantation or before surgery.

Relative costs and availability of the above imaging modalities and local expertise as well as the physician's preference will continue to influence the imaging protocol in different institutions. In our institution, all children with neuroblastoma undergo multimodality imaging for initial staging: CT/MR (including thorax, abdomen and pelvis +/− brain and neck regions) for delineating the extent of primary tumour, MIBG and bone scintigraphy with SPECT for correlation with CT/MR, and the PET study is optional as the cost is covered by the patient's family. Octreotide scintigraphy is not currently available in our centre so the prognosis of neuroblastoma is determined by both clinical staging and pathological classification (Shimada system) [26].

Conclusion

General radiologists and clinicians should be aware of the unusual clinical presentation of neuroblastoma in children. A quick abdominal examination supplemented by ultrasound screening can enable a correct diagnosis while a standardised imaging algorithm can facilitate optimal management of the child.

References

1. David R, Lamki N, Fan S, Singleton EB, Eftekhari F, Shirkhoda A, et al. The many faces of neuroblastoma. Radiographics 1989;9:859–82.
2. Maris JM, Hogarty MD, Bagatell R, Cohn SL. Neuroblastoma. Lancet 2007;369:2106–20.
3. De Bernardi B, Nicolas B, Boni L, Indolfi P, Carli M, Cordero Di Montezemolo L, et al. Disseminated neuroblastoma in children older than one year at diagnosis: comparable results with three consecutive high-dose protocols adopted by the Italian Co-Operative Group for Neuroblastoma. J Clin Oncol 2003;21:1592–601.
4. Lonergan GJ, Schwab CM, Suarez ES, Carlson CL. Neuroblastoma, ganglioneuroblastoma, and ganglioneuroma: radiologic-pathologic correlation. Radiographics 2002;22: 911–34.
5. Lanzkowsky P. Neuroblastoma. In: Lanzkowsky P, editor. Annual of pediatric hematology and oncology. 4 edn. London: Elsevier Academic Press, 2005: 530–2.
6. Matthay KK, Villablanca JG, Seeger RC, Stram DO, Harris RE, Ramsay NK, et al. Treatment of high-risk neuroblastoma with intensive chemotherapy, radiotherapy, autologous

bone marrow transplantation, and 13-cis-retinoic acid. Children's Cancer Group. N Engl J Med 1999;341:1165–73.
7. Sawada T, Hirayama M, Nakata T, Takeda T, Takasugi N, Mori T, et al. Mass screening for neuroblastoma in infants in Japan. Interim report of a mass screening study group. Lancet 1984;2:271–3.
8. Nishi M, Miyake H, Takeda T, Shimada M, Takasugi N, Sato Y, et al. Effects of the mass screening of neuroblastoma in Sapporo City. Cancer 1987;60:433–6.
9. Kaplan SJ, Holbrook CT, McDaniel HG, Buntain WL, Crist WM. Vasoactive intestinal peptide secreting tumours of childhood. Am J Dis Child 1980;134:21–4.
10. Brodeur GM, Pritchard J, Berthold F, Carlsen NL, Castel V, Castelberry RP, et al. Revisions of the international criteria for neuroblastoma diagnosis, staging, and response to treatment. J Clin Oncol 1993;11:1466–77.
11. Ng YY, Kingston JE. The role of radiology in the staging of neuroblastoma. Clin Radiol 1993;47:226–35.
12. Siegel MJ, Ishwaran H, Fletcher BD, Meyer JS, Hoffer FA, Jaramillo D, et al. Staging of neuroblastoma at imaging: report of the radiology diagnostic oncology group. Radiology 2002; 223:168–75.
13. Pfluger T, Schmied C, Porn U, Leinsinger G, Vollmar C, Dresel S, et al. Integrated imaging using MRI and 123I metaiodobenzylguanidine scintigraphy to improve sensitivity and specificity in the diagnosis of pediatric neuroblastoma. AJR Am J Roentgenol 2003;181:1115–24.
14. Sofka CM, Semelka RC, Kelekis NL, Worawattanakul S, Chung CJ, Gold S, et al. Magnetic resonance imaging of neuroblastoma using current techniques. Magn Reson Imaging 1999;17:193–8.
15. Tanabe M, Ohnuma N, Iwai J, Yoshida H, Takahashi H, Maie M, et al. Bone marrow metastasis of neuroblastoma analyzed by MRI and its influence on prognosis. Med Pediatr Oncol 1995;24:292–9.
16. Meyer JS, Siegel MJ, Farooqui SO, Jaramillo D, Fletcher BD, Hoffer FA. Which MRI sequence of the spine best reveals bone-marrow metastases of neuroblastoma? Pediatr Radiol 2005;35:778–85.
17. Howman-Giles R, Bernard E, Uren R. Pediatric nuclear oncology. Q J Nucl Med 1997;41:321–35.
18. Rozovsky K, Koplewitz BZ, Krausz Y, Revel-Vilk S, Weintraub M, Chisin R, et al. Added value of SPECT/CT for correlation of MIBG scintigraphy and diagnostic CT in neuroblastoma and pheochromocytoma. AJR Am J Roentgenol 2008;190:1085–90.
19. Schilling FH, Bihl H, Jacobsson H, Ambros PF, Martinsson T, Borgstrom P, et al. Combined (111)In-pentetreotide scintigraphy and (123)I-mIBG scintigraphy in neuroblastoma provides prognostic information. Med Pediatr Oncol 2000;35:688–91.
20. Orlando C, Raggi CC, Bagnoni L, Sestini R, Briganti V, La Cava G, et al. Somatostatin receptor type 2 gene expression in neuroblastoma, measured by competitive RT-PCR, is related to patient survival and to somatostatin receptor imaging by indium -111-pentetreotide. Med Pediatr Oncol 2001;36:224–6.
21. Pashankar FD, O'Dorisio MS, Menda Y. MIBG and somatostatin receptor analogs in children: current concepts on diagnostic and therapeutic use. J Nucl Med 2005;46 Suppl 1:55S–61S.
22. McHugh K, Pritchard J. Problems in the imaging of three common paediatric solid tumours. Eur J Radiol 2001;37: 72–8.
23. Howman-Giles RB, Gilday DL, Ash JM. Radionuclide skeletal survey in neuroblastoma. Radiology 1979;131: 497–502.
24. Heisel MA, Miller JH, Reid BS, Siegel SE. Radionuclide bone scan in neuroblastoma. Pediatrics 1983;71:206–9.
25. Sharp SE, Shulkin BL, Gelfand MJ, Salisbury S, Furman WL. 123I-MIBG scintigraphy and 18F-FDG PET in neuroblastoma. J Nucl Med 2009;50:1237–43.
26. Shimada H, Ambros IM, Dehner LP, Hata J, Joshi VV, Roald B, et al. The International Neuroblastoma Pathology Classification (the Shimada system). Cancer 1999;86:364–72.